Full-color skin imaging using RGB LED and floating lens in optical coherence tomography

Bor-Wen Yang[1,*] and Xin-Chang Chen[2]

[1]*Department of Opto-electronic System Engineering, Minghsin University of Science and Technology, Hsinchu, Taiwan, 30401*

[2]*Institute of Electronic Engineering, Minghsin University of Science and Technology, Hsinchu, Taiwan, 30401*

**bwyang@must.edu.tw*

Abstract: The cosmetic industry has witnessed significant growth in recent years. Conventional hand-held skin cameras allow for 2D inspection of the skin surface. This paper proposes a new model for full-color 3D imaging of the skin tissue using fiber-based optical coherence tomography (OCT). Compared to laser or LD sources, RGB LED was found more suitable and thus chosen in the low-coherence interferometry due to its wider bandwidth. A floating objective lens was used to confocalize the R, G and B imaging planes and to derive a full-color image of the capillary system in the skin tissue. The skin imaging system can be miniaturized to form a new hand-held model using an RGB integrated source, a micro-interferometer module and a high-speed beam steering device. Non-invasive, full-color and hand-held skin imaging contributes to advances in the fields of skin science, dermatology and cosmetology.

OCIS codes: (170.0170) Medical optics and biotechnology; (170.0110) Imaging systems; (170.4520) Coherence imaging; (170.1870) Dermatology; (170.3880) Medical and biological imaging; (170.4500) Optical coherence tomography

References and links

1. C. J. R. Sheppard, and D. M. Shotton, *Confocal laser scanning microscopy* (Springer, New York, 1997).
2. W. Denk, J. H. Strickler, and W. W. Webb, "Two-photon laser scanning fluorescence microscopy," Science **248**(4951), 73–76 (1990).
3. R. Gauderon, P. B. Lukins, and C. J. R. Sheppard, "Three-dimensional second-harmonic generation imaging with femtosecond laser pulses," Opt. Lett. **23**(15), 1209–1211 (1998).
4. D. Huang, E. A. Swanson, C. P. Lin, J. S. Schuman, W. G. Stinson, W. Chang, M. R. Hee, T. Flotte, K. Gregory, C. A. Puliafito, and J. G. Fujimoto, "Optical coherence tomography," Science **254**(5035), 1178–1181 (1991).
5. J. G. Fujimoto, C. Pitris, S. A. Boppart, and M. E. Brezinski, "Optical coherence tomography: an emerging technology for biomedical imaging and optical biopsy," Neoplasia **2**(1/2), 9–25 (2000).
6. U. Morgner, W. Drexler, F. X. Kärtner, X. D. Li, C. Pitris, E. P. Ippen, and J. G. Fujimoto, "Spectroscopic optical coherence tomography," Opt. Lett. **25**(2), 111–113 (2000).
7. J. Welzel, E. Lankenau, R. Birngruber, and R. Engelhardt, "Optical coherence tomography of the human skin," J. Am. Acad. Dermatol. **37**(6), 958–963 (1997).
8. T. Gambichler, G. Moussa, M. Sand, D. Sand, P. Altmeyer, and K. Hoffmann, "Applications of optical coherence tomography in dermatology," J. Dermatol. Sci. **40**(2), 85–94 (2005).
9. F. Spöler, M. Först, Y. Marquardt, D. Hoeller, H. Kurz, H. Merk, and F. Abuzahra, "High-resolution optical coherence tomography as a non-destructive monitoring tool for the engineering of skin equivalents," Skin Res. Technol. **12**(4), 261–267 (2006).
10. B. W. Yang, L. M. Chan, and K. C. Wang, "The characteristics of three-dimensional skin imaging system by full-colored optical coherence tomography," Opt. Rev. **16**(3), 392–395 (2009).
11. H. Machida, Y. Sano, Y. Hamamoto, M. Muto, T. Kozu, H. Tajiri, and S. Yoshida, "Narrow-band imaging in the diagnosis of colorectal mucosal lesions: a pilot study," Endoscopy **36**(12), 1094–1098 (2004).
12. A. Larghi, P. G. Lecca, and G. Costamagna, "High-resolution narrow band imaging endoscopy," Gut **57**(7), 976–986 (2008).
13. Edison Opto Corporation, Taipei, Taiwan, http://www.edison-opto.com.tw/.
14. T. H. Shao, *Engineering optics: optical design* (Electronic Industry Press, Beijing, 2003).
15. W. F. Cheong, S. A. Prahl, and A. J. Welch, "A review of the optical properties of biological tissues," IEEE J. Quantum Electron. **26**(12), 2166–2185 (1990).

#133669 - $15.00 USD Received 19 Aug 2010; revised 24 Oct 2010; accepted 3 Nov 2010; published 8 Nov 2010

16. A. G. Podoleanu, G. M. Dobre, D. J. Webb, and D. A. Jackson, "Simultaneous en-face imaging of two layers in the human retina by low-coherence reflectometry," Opt. Lett. **22**(13), 1039–1041 (1997).
17. Edison Opto Corporation, Taipei, Taiwan, http://www.walsin.com/.
18. Walsin Lihwa, Taipei, Taiwan, http://www.kaai.com/.
19. Thorlabs, Inc., New Jersey, USA, http://www.thorlabs.us/.
20. Touch Micro-system Technology Corp, Taoyuan, Taiwan, http://www.tmt-mems.com/.

1. Introduction

The cosmetic industry advances extensively in recent years. To inspect the details of face or hand surface, skin cameras employing white source are widely used. Such kind of system can image hairs or pores on skin surface, but can't reveal the capillaries, melanin or collagen distributed within dermal layer. If there is a new system capable of penetrative imaging into skin tissue, customers can trace and prevent the appearance of spots or wrinkles, and may reduce the use of cosmetics and skincare products as well.

All modern imaging technologies have their own advantages and limitations [1–3]. Among them, optical coherence tomography (OCT) has been widely applied because of its non-invasive nature, high spatial resolution [4–6], and the possibility to be modulized and miniaturized. However, the images derived from conventional OCT are typically single-color using infrared (IR) sources [7–9]. This will be challenging to attract the users of skincare products and traditional skin cameras.

The white beam is not intrinsically suitable for OCT imaging due to its broad bandwidth, although division of the white spectrum into three parts, namely, the R, G and B rays with reduced bandwidths, could be suitable for low-coherence interference applications [10]. The application of narrow-band R, G and B rays in gastrointestinal endoscopy can improve the contrast of the derived color images; this is a process known as narrow-band imaging (NBI) [11,12]. A combination of OCT and NBI can make full-color imaging into derm tissue a genuine possibility.

Compared with RGB filters and RGB LD, RGB LED was found more suitable for OCT imaging. Due to imperfect spectrum profile of RGB filters [10] and narrow bandwidth of RGB LD, we chose RGB LED for low-coherence imaging applications. RGB LED possesses merits of broad bandwidth, low cost, long lifetime, small volume, easy maintenance, and ready to be integrated as a multi-color source module. These advantages make it a good candidate for full-color OCT technology.

2. Materials and Methods

To implement the full-color imaging system, we adopted Michelson interferometry to construct a fiber-based OCT configuration, as shown in Fig. 1. Its central portion denotes the optical coupler, which forms the interferometry core. The top right shows the RGB LED sources and related optics. Driven by a current of ~1.35 A, each of the LEDs delivers a flux of ~350 lm [13]. The bottom right portion of Fig. 1 shows the sample arm, which is used to scan the sample during the imaging process. This arm consists of a GRIN lens for collimation and an objective lens to focus the scan beam. The interference signal is received by an optical detector and subsequently transferred to a computer system for image processing.

#133669 - $15.00 USD Received 19 Aug 2010; revised 24 Oct 2010; accepted 3 Nov 2010; published 8 Nov 2010

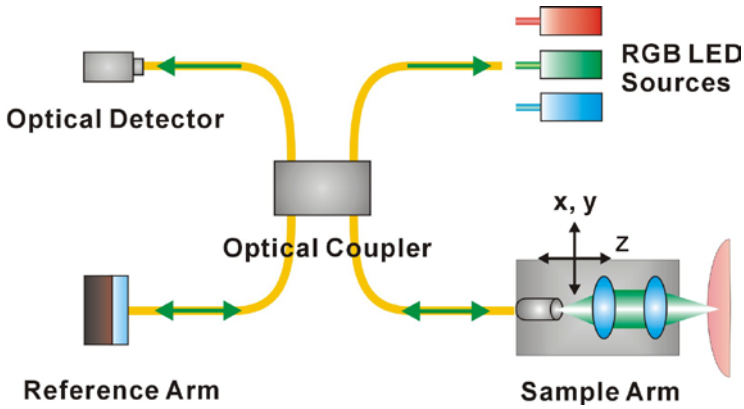

Fig. 1. The OCT system for full-color imaging.

As an example, when we light the red LED to scan the tissue, the OCT system detects the back-scattered red light from the scanned point to interfere with the red beam incident from the reference arm. The intensity of this red interference signal is proportional to that of the red light scattered from the scanned point, which is exactly the red content while the sampled point is seen by human eyes. Our system uses self-developed LabVIEW^{TM} program to transform the time-resolved interference signal into a red single-color image, as shown in Fig. 2(a). This program transforms the interference signal (top right block) into a real-time red image (bottom right block), and finally into a completed R, G, or B image (bottom left block); the top left block indicates the panel used to control the scanning motion of sample arm. Figure 2(b) demonstrates the program used to overlap the R, G, and B single-color images (shown in the middle row) to form a full-color image (top right block); accordingly, this combined image reveals the contours and colors of the scanned tissue as seen by human eyes.

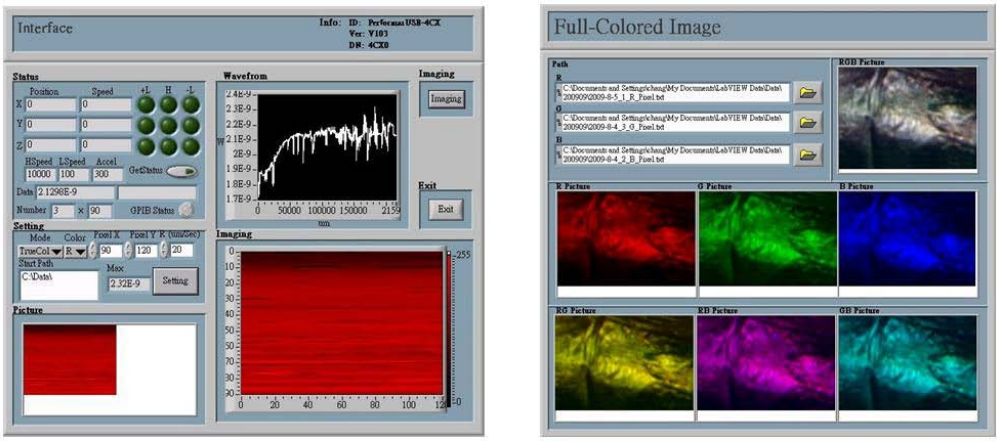

a b

Fig. 2. (a) The LabVIEW^{TM} program used to transform the interference signal into a real-time image and a completed R, G, or B image; (b) The LabVIEW^{TM} program used to overlap the R, G, and B images to form a full-color RGB image.

3. Results and discussion

In this study, we applied RGB LED in a fiber-based OCT system for skin imaging. Due to the separation of R, G, B focal planes, a floating objective lens was equipped to achieve the confocal requirement. Overlapping three R, G and B single-color images, we demonstrated a combined en-face image of micro-capillaries in derm tissue. We then apply modern

#133669 - $15.00 USD Received 19 Aug 2010; revised 24 Oct 2010; accepted 3 Nov 2010; published 8 Nov 2010

micro-opto-electromechanical system (MOEMS) technology to design a new skin imaging system incorporating RGB integrated source module, micro-interferometry and high-speed scanning mirror into a personal and portable model.

3.1 Penetration depth and resolutions

The penetration depth and spatial resolutions of the R, G and B rays are summarized in Table 1, where the penetration depth, lateral and axial resolutions are derived by $1/(\pi f\mu_0\sigma)^{1/2}$, $2\lambda/(\pi NA)$ and $2(\ln 2)\cdot\lambda^2/(\pi\Delta\lambda)$, respectively. In these calculations, the peak wavelengths (λ_p) and FWHMs ($\Delta\lambda$) of the beams are listed as follows: red: $\lambda_p = 640$ nm, $\Delta\lambda = 15$ nm; green: $\lambda_p = 525$ nm, $\Delta\lambda = 30$ nm; blue: $\lambda_p = 450$ nm, $\Delta\lambda = 19$ nm. As shown in Table 1, the penetration depth ranges from 0.64 to 0.76 mm, sufficient for imaging the main organs in skin tissue [7].

Table 1. The penetration depth (A), lateral (B), and axial (C) resolutions of the R, G and B rays, respectively

	A	B	C
Red LED	0.758 mm	0.679 μm	12.05 μm
Green LED	0.686 mm	0.557 μm	4.054 μm
Blue LED	0.636 mm	0.477 μm	4.703 μm

As the R, G, and B scanning beams are focused onto different imaging planes, the objective lens should be dynamically shifted towards or away from the sample surface to achieve con-focalization for ideal image superimposition. For an altered distance A between the objective lens and the sample surface, the focusing depths B_1, B_2, and B_3 of the blue, green and red beams, respectively, were derived by TracePro™ modeling, as illustrated in Fig. 3. The modeled objective lens has a magnification of 20x, a numerical aperture of 0.40 and a focal length of 6.89 mm [14]. The index and thickness of the epidermis are 1.335 and 0.2 mm, respectively, and those of the dermis are 1.37 and 0.6 mm, respectively [15]. The simulation results have been summarized in Table 2.

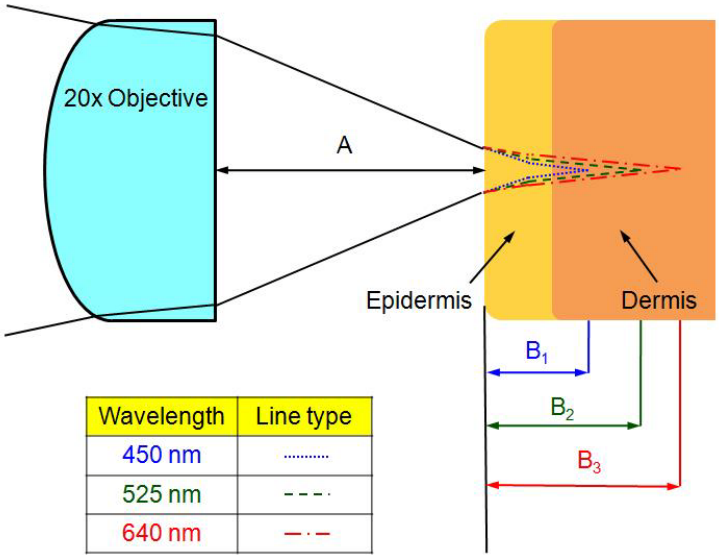

Fig. 3. Modeling using TracePro™ to derive the focusing depths of the B, G and R beams incident on sample skin.

#133669 - $15.00 USD Received 19 Aug 2010; revised 24 Oct 2010; accepted 3 Nov 2010; published 8 Nov 2010

Table 2. The dependence of the focusing depths of the B, G and R rays (B_1, B_2 and B_3) on the distance between the objective lens and the sample surface (A)

A	B_1	B_2	B_3
0.70 mm	0.5616 mm	0.6557 mm	0.7462 mm
0.72 mm	0.5333 mm	0.6259 mm	0.7190 mm
0.75 mm	0.4906 mm	0.5847 mm	0.6762 mm
0.79 mm	0.4386 mm	0.5327 mm	0.6242 mm
0.80 mm	0.4197 mm	0.5144 mm	0.6055 mm
0.85 mm	0.3488 mm	0.4430 mm	0.5363 mm
0.90 mm	0.2790 mm	0.3739 mm	0.4627 mm

3.2 En-face scanning and full-color imaging

Choosing a red beam of λ_p = 640 nm, we first shifted the objective lens so that the distance A between the objective and skin surface became 0.85 mm. From Table 2, the focusing depth B_3 of the red beam was found to be 0.5363 mm. Using en-face scanning to derive image parallel to the sample surface [16], the red image of the skin tissue was obtained, as shown in Fig. 4(a). Using a green beam of λ_p = 525 nm, the objective lens was shifted so that the distance A = 0.79 mm. The focusing depth B_2 was found to be 0.5327 mm, as shown in Table 2, and the resulting green image is depicted in Fig. 4(b). By a blue beam of λ_p = 450 nm, we made A = 0.72 mm, B_1 = 0.5333 mm and retrieved the blue image shown in Fig. 4(c). Every image in Fig. 4 consists of 160 × 120 pixels, each having a size of 20μm × 20μm. A combination of the R, G, B images yields a full-color image, which shows the details of a capillary structure, as illustrated in Fig. 5.

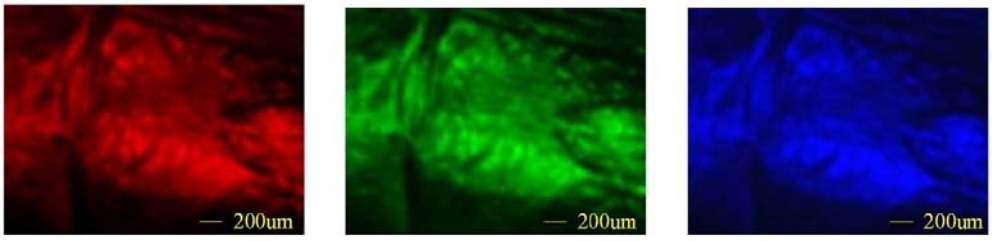

Fig. 4. The R, G and B images derived from the skin imaging system.

Fig. 5. A combined image of the capillary system in skin tissue.

3.3 Miniaturization to a hand-held model

To extend its applications to common users, the full-color imaging system has also been designed as a hand-held model, as depicted in Fig. 6. The light source, capable of multi-color illumination, is composed of an RGB LED source module [17,18]. The emitted R, G and B lights are directed towards the interferometer module [19] to achieve low-coherence

#133669 - $15.00 USD Received 19 Aug 2010; revised 24 Oct 2010; accepted 3 Nov 2010; published 8 Nov 2010

interference. The micro-actuated scanning mirror deflects the beam into the sample to enable tissue scanning and imaging [20]. The detection module transforms the signal stream into pixel brightness for image reconstruction.

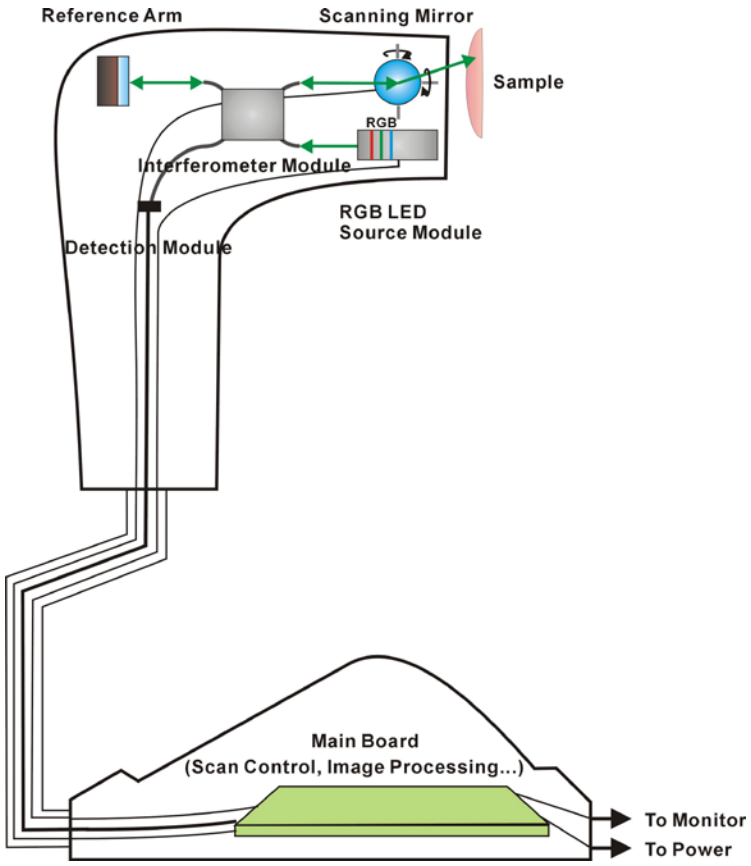

Fig. 6. A design of hand-held model for the full-color skin imaging system.

Among the key components mentioned above, RGB integrated source module and micro-actuated scanning mirror belong to the main parts of a laser scanning micro-projector, and the interferometer module is early commercialized. Therefore, the hand-held 3-dimensional skin imaging system is promising in the future. Academically, it can contribute to the dermatology and skin medicine; commercially, it may help to promote the cosmetology and anti-aging market.

4. Conclusion

By a combination of OCT and NBI technologies, we proposed a new skin imaging technique to improve the penetration power of general skin camera system. Division of white spectrum into R, G and B sub-ranges was simultaneously applicable to OCT and full-color applications. Among RGB source candidates, we found RGB LED the most suitable for full-color OCT system. The R, G and B images from identical tissue cross-section were derived by a floating objective lens. Overlapping the three images produced a full-color image of the skin tissue. The imaging system can be miniaturized to a hand-held model by applying MOEMS technology. Being non-invasive, full-color and hand-held, the new skin imaging system shows great potential in the applications of skin science, dermatology and cosmetology.

#133669 - $15.00 USD Received 19 Aug 2010; revised 24 Oct 2010; accepted 3 Nov 2010; published 8 Nov 2010